1 **Seasonal and vertical dynamics in the trophic structure of a temperate zooplankton**

2 **assemblage**

3 Sonia Romero-Romero*[1,a], Ricardo González-Gil[2], Carlos Cáceres [2,b], José Luis Acuña[1]

4 [1] Área de Ecología, Dpto. de Biología de Organismos y Sistemas, Universidad de Oviedo,

5 Catedrático Rodrigo Uría s/n, 33071 Oviedo, Asturias, Spain

6 [2] Department of Mathematics and Statistics, University of Strathclyde, Glasgow, UK

7 [a] Present address: University of Hawaii at Manoa, Department of Oceanography, 1000

8 Pope Road, Honolulu, Hawaii, 96822, USA

9 [b] Present address: Schiermeier Olentangy River Wetland Research Park, School of

10 Environment and Natural Resources, The Ohio State University, Columbus, USA

11

12 *Corresponding author: romeroromerosonia@gmail.com

13 **Running head:** Trophic structure of zooplankton

14

15   **Abstract**

16   We determined the stable nitrogen isotope composition (δ^{15}N values) and body size

17   of taxonomic groups in a zooplankton community in the Cantabrian Sea (southern Bay of

18   Biscay) to explore seasonal and depth (0-2000 m) variations in the size-based trophic

19   structure, and their coupling to the production cycle. The positive linear relationship

20   between δ^{15}N values and log-transformed body size reflects the dominance of new vs.

21   regenerated production. The slope of the relationship (*b)* is high during productive periods

22   and low when herbivory declines and the food web is more dependent on recycled

23   production. This variation can be attributed to high δ^{15}N values of the smallest plankton

24   after repetitive cycles of microbial degradation. Downward transport of organic matter after

25   the spring phytoplankton bloom was captured by a steady variation from low values of *b* at

26   the surface to high values at the bathypelagic zone, where the imprint of the spring

27   production pulse could still be detected. Variation in *b* reveals that the meso- and

28   bathypelagic zooplankton communities are as dynamic as their epipelagic counterparts.

29   This shows the efficiency of δ^{15}N vs. body size relationships to capture fast, transient

30   ecosystem processes without need for lengthy incubations or complex rate measurements.

31

32   **Keywords**: deep-sea, stable isotopes, size-based

33

Introduction

34

35   Deep benthic communities depend on a "rain" of organic matter (OM) produced at

36   the surface of the ocean and transported downwards by a combination of mechanisms

37   known as the "biological pump" (Turner 2015). To reach the deep ocean floor, the OM

38   must go through the mesopelagic zone, where nearly 90% of the exported carbon is

39   respired (Arístegui et al. 2005). Passively sinking particulate organic carbon is regarded as

40   the main source of organic carbon to the deep-sea. However, zooplankton alter the carbon

41   flux by consuming and metabolizing sinking or suspended particles and by fragmenting

42   large aggregates (Dilling and Alldredge 2000), or by repackaging the ingested particles into

43   fecal pellets (Wilson et al. 2008). In addition, they perform diel vertical migrations, which

44   contribute to the rapid descent of fecal pellets, molts, and dead carcasses to deeper portions

45   of the water column (Steinberg et al. 2008; Burd et al. 2010). Zooplankton also represent

46   the trophic link between phytoplankton and higher trophic levels (Hannides et al. 2009),

47   thus a change in the trophic structure of zooplankton may potentially affect the entire food

48   web. Although the structure and dynamics of zooplankton are of major importance to the

49   functioning of deep-sea ecosystems, their study, especially in the deep-sea, has been

50   hindered by sampling constraints at representative time and space scales (Robinson et al.

51   2010).

52   Seasonal fluctuations in primary production, especially accentuated in temperate

53   seas with a marked annual cycle, are determinant for the dynamics of the deep ocean

54   (Gooday 2002). In these temperate regions, the transition from mixed to stratified

55   conditions in spring and back to mixing in autumn releases phytoplankton cells from

56   light/nutrient limitation, leading to two major production pulses known as the spring and

57   autumn blooms, respectively (e.g. Fernández and Bode 1991; González-Gil et al. 2018).

58   Stratification favors the prevalence of a microbial food loop (Cushing 1989; Legendre and

59   Rassoulzadegan 1995), where heterotrophic bacteria recycle the organic matter while

60   feeding a complex community of heterotrophic or mixotrophic microbes, protozoans and

61   copepods (Azam et al. 1983). In contrast, during blooms, the production depends on

62   phytoplankton (Cushing 1989), and the organic matter produced is either efficiently

63   transferred to upper trophic levels in a few trophic steps or rapidly sinks to the deep ocean.

64   Due to difficulties in experimentation and rate measurements at great depths, the impact of

65   seasonal fluctuations in the primary production of the euphotic layer on the trophic

66   structure of deep zooplankton communities remains poorly known.

67   Stable isotopes are widely used as tracers in studies of trophic ecology to provide

68   information on the origin of organic matter and its transfer through the food web (e.g.

69   Boecklen et al. 2011 and references therein). Stable nitrogen isotope values (as δ^{15}N values)

70   are used to estimate the relative trophic level of organisms since they increase ~3-4 ‰

71   between a predator and its prey (Minagawa and Wada 1984). Additionally, for primary

72   producers, it also informs about the origin of the assimilated nitrogen by organisms.

73   Because of its short tissue turnover rate, the variability in the δ^{15}N values of zooplankton

74   have a marked seasonal component (Rolff 2000; Matthews and Mazumder 2005). Seasonal

75   variations have also been described for the stable isotope composition of deep-sea

76   zooplankton (Fanelli et al. 2011), pointing to a connection between surface dynamics and

77   deep zooplankton communities. In this regard, Laakmann and Auel (2010) indicated that

78   regional changes in surface stable isotope values propagate to deep layers and are reflected

79   in deep-sea carnivorous copepods. Moreover, previous studies on the stable isotope

80   composition of zooplankton have described an increase in $\delta^{15}N$ values with depth

81   (Koppelmann 2003; Koppelmann et al. 2009; Hannides et al. 2013). However, there is a

82   lack of studies addressing seasonal variations in the isotopic composition of zooplankton

83   simultaneously at different depths.

84   Size-based analyses provide information about the structure and function of a food

85   web (Cohen et al. 1993; Jennings and Dulvy 2005; Woodward et al. 2005), since body size

86   is a key attribute related to many life-history traits (Peters 1983). For instance, predators are

87   usually larger than their prey (Sheldon et al. 1972), which explains why the body size of

88   organisms accounts for more variation in their trophic position than their taxonomic

89   identity (Jennings et al. 2008a). Previous studies have quantified the relationship between

90   body size and trophic level in marine ecosystems using analyses of stable isotopes, and

91   most assumed that the dependence of trophic level on body size is constant through time

92   (e.g. Jennings et al. 2002; Al-Habsi et al. 2008), although there are few investigations

93   where temporal variations were considered (e.g. Jennings et al. 2007; Nakazawa et al.

94   2010; Romero-Romero et al. 2016a). This relationship is expected to be stronger in marine

95   food webs which are based on phytoplankton than those dependent on detritus (Layman et

96   al. 2005; Al-Habsi et al. 2008). If that holds true, dependence of new versus recycled

97   production, which vary during the annual cycle of nutrients, could be reflected in the

98   strength of the relationship between $\delta^{15}N$ values and body size, when organisms with short

99   tissue turnover rates are analyzed. However, food web studies using stable isotopes have

100   traditionally been limited to larger-sized organisms (Middelburg 2014) because the analysis

101   of the stable isotope composition of zooplankton requires a pool of organisms, so samples

102   are commonly analyzed according to their size binned in size fractions. This restricts the

103   analysis to typically four or five discrete size classes (e.g. Rolff 2000; Hannides et al.

104   2013), preventing the use of size-based approaches.

105   In this study, we analyzed seasonal variations throughout the water column in the

106   δ^{15}N values of zooplankton according to their taxonomic group. We used a body size-based

107   approach to quantify changes in the dependence of the zooplankton food web in the

108   Cantabrian Sea (southern Bay of Biscay) on new versus recycled production. We

109   hypothesized that the relationship between δ^{15}N values and body size would be stronger

110   during the spring phytoplankton bloom than during the stratification period and that

111   seasonal variations would be less marked at greater depths.

112

113   **Materials and Methods**

114   *Sampling methods* – The study area extended from 44°23' to 43°56' N and from

115   6°31' to 5°47' W (Fig. 1) over the Avilés submarine canyon, which is part of a complex

116   network of canyons and valleys off the Central Cantabrian margin in the Bay of Biscay

117   (Northern Iberian Peninsula; Gómez-Ballesteros et al. 2014). Samples were collected on

118   board the research vessel B/O Sarmiento de Gamboa during three oceanographic cruises:

119   between 3 and 13 March 2012 (BIOCANT1); between 27 September and 6 October 2012

120   (BIOCANT2) and between 24 April and 4 May 2013 (BIOCANT3). During each cruise we

121   sampled at five different stations: C3, C5, C8, TP and P3 as well as at station C6 during

122   BIOCANT3 (Fig. 1), and obtained profiles of temperature, salinity and fluorescence by

123   means of a Seabird911- plus CTD probe. Water samples for the measurement of

124   chlorophyll *a* (Chl *a*) and particulate organic matter (POM) were collected using Niskin

125   bottles at depths of 5, 25, 50, 75, 100, 200, 300, 500 m, and then every 500 m down to the

126   seafloor at each station (n = 201). Mesozooplankton was collected by oblique tows of a 1

127   m^2 Multiple Opening/Closing Net and Environmental Sensing System (MOCNESS)

128   equipped with 8 nets of 200 µm mesh size. Tow intervals for the MOCNESS were defined

129   according to the water mass structure (Botas et al. 1989), as depicted in the CTD profiles:

130   1) Surface Water (SW), which coincides with the mixing layer from 0-200 m depth; 2)

131   North Atlantic Central Water (NACW), from 200 m to the salinity minimum located

132   around 400-500 m depth; 3) Mediterranean Water (MW), which goes down to around 1200

133   m depth when a salinity of 35.6 is reached; and 4) Transition Water (TW), which is a

134   mixture between MW and deep water and it was sampled only at the deepest stations (C5,

135   C6 and C8) down to 2000 m (Fig. 1).

136   *Sample processing and stable isotope analyses* – Water samples for the analyses of

137   suspended POM were prefiltered through a 100 µm mesh sieve to remove

138   mesozooplankton, filtered through 25 mm Whatman GF/F filters and stored frozen at -

139   20°C. Each mesozooplankton sample was divided into two halves using a Motoda splitter,

140   one half was fixed in a 4% formaldehyde sea-water buffered solution and the other half was

141   transferred to Whatman glass-fiber GF/A filters and immediately stored frozen at -20°C.

142   For stable isotope analyses, each zooplankton sample was first thawed and then

143   fractionated through a 500 µm mesh sieve to separate the 200-500 µm size class that was

144   processed as a single sample. Then, individuals larger than 500 µm were sorted according

145   to their taxonomic group and, when possible, 6 to 10 groups from each water mass within

146   each sampling station were separated. Most specimens were determined to genus level

147   (Supporting Information Table S2). To obtain sufficient sample material for stable isotope

148   analysis, several individuals of similar size belonging to the same taxonomic group were

149   pooled together. All individuals within a sample were photographed together under a

150   stereoscopic microscope. From the pictures taken, we determined the mean body length of

151   each sample using the image analysis software ImageJ (Abràmoff et al. 2004) and

152   calculated body mass using length/weight conversion factors available in the literature

153   (Company and Sardà 2000, for decapods; Färber-Lorda 1994, for euphausiids; and Uye

154   1982 for copepods, ostracods, cladocerans and chaetognaths).

155   Prior to isotopic analysis, all POM and zooplankton samples were dried at 60°C for

156   48 h. We did not extract lipids from the samples since lipid extraction has been reported to

157   have little effect on $\delta^{15}N$ values of aquatic organisms (Ingram et al. 2007). After drying,

158   GF/F filters were packed in 5×9 mm tin capsules. Zooplankton samples were ground to a

159   fine powder using pestle and mortar and packed in 3.3×5 mm tin capsules. All samples (n=

160   544) were processed in a Thermo Finnigan Mat Delta Plus isotope-ratio mass spectrometer

161   coupled to a Carlo Erba CHNSO 1108 elemental analyzer in the Unidad de Técnicas

162   Instrumentales de Análisis (A Coruña, Spain). ^{15}N abundance is expressed in δ notation as

163   the deviation from the standard in parts per thousand (‰) according to the following

164   equation:

165        $\delta^{15}N = [(R_{sample}/R_{standard})-1] \times 1000$,

166   where R is the ratio $^{15}N/^{14}N$ and the $R_{standard}$ values were based on atmospheric N_2.

167   Measurements of internal laboratory standards glutamic acid (USGS40, USGS41) and L-

168   alanine (IA R041) every 16 samples indicated measurement errors of $\pm$ 0.1, 0.2 and 0.14‰

169   for $\delta^{15}N$, respectively.

170   *Data analysis* – To determine the influence of depth and season on the size-based

171   trophic structure we fitted linear mixed effects models. The fitted models were nested in a

172   global model (i.e. highest-dimensioned) that included $\delta^{15}N$ as dependent variable, body size

173   (W) as covariate, depth strata (SW, NACW, MW and TW) and cruise (March 2012,

174   October 2012 and May 2013) as fixed factors, and taxonomic group as random factor

175   (Supporting Information). We used linear mixed effects models to take into account

176   variation due to taxonomic identity, included as random factor. Data from the smallest

177   zooplankton size fraction (200-500 µm) was excluded from the analysis because it

178   integrated a wide size range. We then followed a top-down model selection approach as

179   recommended by Zuur et al. (2009) and ranked models according to their second-order

180   Akaike Information Criterion (AICc). The conditional R^2 value (i.e. variance explained by

181   both fixed and random factors) was calculated following Nakagawa and Schielzeth (2013).

182   We defined the $\delta^{15}N$ values at the base of the studied food web as the predicted $\delta^{15}N$

183   for organisms weighing 10^{-4} g from each fitted regression line of the best model. We also

184   analyzed, for those taxonomic groups present in all three BIOCANT cruises, the

185   relationship between their range of variation of $\delta^{15}N$ values among seasons (i.e. highest

186   minus lowest mean $\delta^{15}N$ values) and their mean body size. We performed all statistical

187   analyses using R, version 3.1.3 (R Core Team 2015) and we used the *lme4* package (Bates

188   et al. 2014) to fit the linear mixed models.

189
190   **Results**

191   *Depth changes in the stable isotope composition of size-fractionated zooplankton* –

192   We determined the δ^{15}N values of 343 samples belonging to 39 taxonomic groups

193   (Supporting Information Table S1). The δ^{15}N values of zooplankton, averaged for all size

194   fractions, increased significantly with depth (from SW to TW) for all three cruises

195   irrespective of the sampling station (ANOVA; March: $F_{1,118} = 89.6$, $p < 0.001$, n=120;

196   October: $F_{1,101} = 4.41$, $p = 0.001$, n=103; May: $F_{1,118} = 14.64$, $p < 0.001$, n=120; Fig. 2),

197   with the highest increase during March (BIOCANT 1; 4.1–9.9‰). In October (BIOCANT

198   2), there was a smaller increase of δ^{15}N values with depth (6.6–8.0‰), however

199   zooplankton had on average higher δ^{15}N values than in March, mainly within SW (0-200

200   m). In May (BIOCANT 3), δ^{15}N values increased with depth especially for those organisms

201   >5.0 mm (5.9–10.9‰). For all three cruises, there was also a trend towards higher δ^{15}N

202   values with size fraction within each water mass (Fig. 2). The δ^{15}N values of suspended

203   POM also generally increased with depth, especially in the upper 300 m. However, in

204   March, δ^{15}N values of suspended POM below 500 m were depleted in ^{15}N in relation to

205   surface waters and differed markedly from that of zooplankton. In contrast, in May the δ^{15}N

206   values of suspended POM were similar to those of the smallest zooplankton size fractions

207   throughout the water column.

208   *Size-based trophic structure* – The best linear mixed model explained a variance of

209   80%, and included: body size as covariate; season and depth as fixed factors, with a

210   different slope and intercept for each level of a factor (i.e. triple interaction between body

211   size, season and depth); and taxonomic group as random factor affecting the intercept

212   (Supporting Information Table S3). The results from the best model are shown in Figures 3

213   and 4. In March, the slope of the δ^{15}N vs. $\log_{10}$ W relationship (*b)* was highest in SW and

214   shallower at higher depths. The opposite was true in May, when *b* was shallowest at SW

215   and increased towards the deep TW. In contrast, in October *b* was mainly constant

216   throughout the water column. The predicted δ^{15}N values for organisms at the base of the

217   studied food web (i.e. organisms weighing 10^{-4} g) increased markedly with depth in March,

218   whereas in October and especially in May they remained nearly invariant, being higher in

219   October (Fig. 4). Seasonal fluctuations in the δ^{15}N values of taxonomic groups were

220   negatively correlated to their body size (δ^{15}N = 0.19 - 0.68 $\log_{10}$ W; R^2 = 0.31; p = 0.01; n =

221   18; Supporting Information Fig. S2). Hence, smaller organisms exhibited higher seasonal

222   variations in δ^{15}N values.

223   **Discussion**

224   Our results implied that the onset of nutrient regeneration leaves a clear imprint on

225   the size-based trophic structure of the zooplankton community in a deep oceanic water

226   column. The lack of structure, as revealed by a flat δ^{15}N vs $\log_{10}$ body size line, which is

227   characteristic of a recycling state, appeared at the surface following the spring production

228   peak, and propagated downward following an orderly sequence which could be readily

229   identified at surprisingly short time-scales (Figs. 3 and 4). Certainly, seasonal patterns in

230   the stable isotope composition of zooplankton have previously been described (e.g. Rolff

231   2000; Matthews and Mazumder 2005; Kürten et al. 2013; Espinasse et al. 2014), including

232 variations in the relationship between δ^{15}N values and size in epipelagic zooplankton (Rolff

233 2000). However, ours is the first evidence of seasonal changes in the size-based trophic

234 structure along a depth gradient.

235   The BIOCANT cruises are representative of three different environmental

236 conditions, which were previously described in Romero-Romero et al. (2016a; Table 1;

237 Supporting Information Fig. S1). Conditions during BIOCANT 1 (March 2012) were

238 typical for the onset of the spring phytoplankton bloom, with high concentrations of Chl *a*

239 that reflected the high, newly produced phytoplankton biomass (González-Gil et al. 2018).

240 During that period, the food web in SW was highly size-structured, as shown by the high *b*

241 (2.37 ‰ g^{-1}; Fig. 3a), suggesting that the herbivorous food web was the dominant trophic

242 pathway in SW. Assuming a constant trophic fractionation of 3.4‰ (Minagawa and Wada

243 1984), the predator: prey body mass ratio (PPMR) in size-structured food webs can be

244 calculated from *b* as PPMR = $10^{(3.4/\,b)}$ (Jennings et al. 2002), yielding a value of 27:1. This

245 PPMR calculated for zooplankton is two orders of magnitude lower than mean estimates

246 for the entire ecosystem from copepods to top predators (~10^3:1; Romero-Romero et al.

247 2016a). This might be explained by the fact that PPMR increases with predator size (Barnes

248 et al. 2010) and our analysis was focused only on a narrow size range not including larger

249 organisms. In contrast to the situation in SW, the food web in deeper water masses was less

250 structured because most of the newly produced organic matter in SW had not yet started to

251 sink (Romero-Romero et al. 2016b). Hence, the OM available below SW was scarce and

252 more refractory, probably forcing primary consumers to broaden their diet. It is important

253   to highlight that in TW in March only four samples were analyzed, therefore the slope of

254   the fitted regression line might not represent an actual pattern.

255   Contrary to the bloom situation, BIOCANT 3 (May 2013) corresponded to an early

256   stratification period (Table 1) during which the food web was unstructured in SW but,

257   became progressively size-structured deeper in the water column (Fig. 3b). Phytoplankton

258   biomass in SW during this cruise had already declined after the 2013 spring bloom (Rumín-

259   Caparrós et al. 2016), so herbivory was likely limited. A shallower b was probably the

260   result of opportunistic feeding by the larger organisms on microzooplankton or small-sized

261   particles when food is scarce (Fry and Quiñones 1994). Conversely, as a consequence of

262   the arrival of material produced during the phytoplankton bloom at greater depths, food was

263   plentiful and b was steeper at TW (2.29 ‰ g^{-1}; Fig. 3b). Likewise, Koppelmann et al.

264   (1999) explained an increase in mesozooplankton biomass in the bathypelagic zone of the

265   NE Atlantic from spring to summer as a consequence of the arrival, at that great depths, of

266   material produced during the phytoplankton bloom. Our results show that the arrival of that

267   material to the deep ocean has also implications for the trophic structure of the bathypelagic

268   zooplankton food web.

269   During BIOCANT 2 (October 2012), which corresponded to a late stratification

270   period (Table 1), the food web was weakly size-structured across the entire water column

271   (Fig. 3c). This concurs with lower mass fluxes to the seafloor than in spring (Rumín-

272   Caparrós et al. 2016) and limited primary production, which leads to a food web mainly

273   dependent on recycled production. In addition, it is precisely in these conditions that the

274   diel vertical migrations of zooplankton are more active (Takahashi et al. 2009), what would

275 lead to vertical homogenization. Interestingly, we found that the mesopelagic community,

276 occupying NACW and MW, exhibited a more time-invariant size structure than the epi-

277 and bathypelagic communities. Vertical migrations are mainly conducted by mesopelagic

278 fauna that transport OM from the epipelagic to the mesopelagic zone (Angel and Baker

279 1983). This may represent a mean to fulfil metabolic carbon requirements in the food-

280 limited mesopelagic zone (Steinberg et al. 2008), and leads us to hypothesize that the

281 mesopelagic zone is seasonally more stable due to vertical migration. Another factor

282 contributing to the relative stability in the size structure of the mesopelagic community

283 might be the typically fast sinking fluxes resulting from high production episodes. The bulk

284 of those fluxes probably reach the benthic system, while mostly bypassing the mesopelagic

285 community (Honjo et al. 1982; Deuser 1986).

286   Marine plankton communities are usually considered highly structured by size due

287 to scale-dependent processes and constraints on the relative masses of predators and their

288 prey (Sheldon et al. 1977; Jennings et al. 2008a). However, there are clear indications that

289 some of the seasonal variation may in fact be due to changes in the species composition

290 (Bode and Alvarez-Ossorio 2004). For this reason, we have applied a mixed modelling

291 approach that accommodates variation due to taxonomic identity into a coherent statistical

292 framework. For example, the deep copepod *Lucicutia* spp. exhibited consistently high and

293 positive residuals from the $\delta^{15}N$ vs. $\log_{10} W$ relationship. Their high mean $\delta^{15}N$ value (10.8

294 ± 0.8‰; Supporting Information Table S2) agrees with that of *Lucicutia longiserrata* in the

295 Mediterranean (11.9‰; Koppelmann et al. 2009), which have been explained by a diet

296 including suspended rather than sinking POM (Gowing and Wishner 1998). In our study,

297   the mean δ^{15}N values of suspended POM below SW (200 m) were 6-7‰ in May and

298   October (Fig. 2), corresponding to a difference of one trophic level with *Lucicutia* spp.

299   However, the nitrogen stable isotope composition of faster sinking particles collected in

300   sediment traps, deployed from March 2012 to March 2013 in the study area, was on

301   average 4.3 ± 0.2‰ (Romero-Romero et al. 2016b), thus lending support to a diet based

302   preferentially on suspended POM.

303   Apart from the variability in the strength of size structuring, there were also marked

304   variations of δ^{15}N values at the base of the studied food web (i.e. smallest zooplankton, Fig.

305   4). Because of their shorter tissue turnover times, smaller organisms are expected to exhibit

306   wider seasonal variability in their stable isotope composition (O'Reilly and Hecky 2002),

307   which is confirmed by observations of a negative correlation between the seasonal range of

308   variation in δ^{15}N values and body size (Jennings et al. 2008b; Supporting Information Fig.

309   S2). During the onset of the spring bloom (March), δ^{15}N values of small zooplankton

310   increased significantly with depth (Fig. 4). This matches the described pathways of OM in

311   the study area, with fresh OM available in SW and old, refractory OM that has suffered

312   several cycles of microbial degradation in deeper water masses (Romero-Romero et al.

313   2016b). If the microbial food loop prevails at the base of the food web, small zooplankton

314   is expected to have higher δ^{15}N values (Saino and Hattori 1980; Mintenbeck et al. 2007).

315   However, in the early stratification period (May), δ^{15}N values of the smaller organisms

316   were nearly constant with depth. This is likely due to the presence of relatively fresh

317   organic material left by a wave of sinking biomass travelling across all depths after the

318   spring bloom. During late stratification (October), δ^{15}N values of small zooplankton were

319   also similar at all depths, but higher than during the early stratification period, which points

320   to a diet more dependent on recycled production as stratification progresses (Bănaru et al.

321   2013). An interesting pattern in our results was that the slope of the δ^{15}N vs. $\log_{10}$ W

322   relationship appeared to be constrained by the δ^{15}N values at the base of the studied food

323   web (Fig. 4). In other words, when small zooplankton had high δ^{15}N values, the food web

324   was always weakly size-structured. However, if δ^{15}N values of small zooplankton were low

325   the food web tended to be more size-structured because fresh OM was available. Thus, it

326   seems that the degree of size structuring of a food web depends on the dominant trophic

327   pathway (Supporting Information Fig. S3).

328   The δ^{15}N values of zooplankton are known to increase with depth, a pattern that has

329   been well grounded on studies in the North Pacific (4.6‰ from 0-1000 m; Hannides et al.

330   2013), the Mediterranean Sea (~7‰ from 0-4000 m; Koppelmann et al. 2009) or the South

331   Atlantic Ocean (6.9‰ from 0-1600 m; Laakmann and Auel 2010) and is also evident in our

332   results (up to 5.8‰ during the onset of the phytoplankton bloom, from 0-2000 m, Fig. 2).

333   This has been attributed to either a ^{15}N enrichment at the base of the food web or a higher

334   trophic level of deep water organisms (Polunin et al. 2001; Hannides et al. 2013).

335   According to our results, both explanations may hold, depending on the recycling state of

336   the system, with the first explanation applying to old regenerative systems (i.e. deep water

337   masses during the onset of the spring phytoplankton bloom) and the second applying to

338   systems which have recently received inputs of fresh OM (i.e. deep water masses during

339   early stratification).

340   **Conclusions**

341   In summary, our size-based approach using stable isotopes reveals seasonal and

342   vertical changes in the trophic structure of a zooplankton food web at short time-scales,

343   reflecting its coupling with the seasonal cycle of primary production and the transfer of OM

344   to the deep-sea. We demonstrate that meso- and bathypelagic zooplankton communities can

345   be as dynamic as their epipelagic counterparts, and exhibit seasonal variations tightly

346   coupled to the particle flux. Our results also provide strong indication that the size-based

347   trophic structure of zooplankton communities reflects the dominance of new vs.

348   regenerated production within the ecosystem and the time elapsed since the onset of

349   regeneration.

361   **References**

362   Abràmoff, M. D., P. J. Magalhães, and S. J. Ram. 2004. Image processing with imageJ.

363   Biophotonics Int. **11**: 36–41.

364   Al-Habsi, S., C. Sweeting, N. Polunin, and N. Graham. 2008. δ^{15}N and δ^{13}C elucidation of

365   size-structured food webs in a Western Arabian Sea demersal trawl assemblage. Mar.

366   Ecol. Prog. Ser. **353**: 55–63. doi:10.3354/meps07167

367   Angel, M. V, and A. D. C. Baker. 1983. Vertical distribution of the standing crop of

368   plankton and micronekton at three stations in the northeast Atlantic. Deep Sea Res.

369   Part B. Oceanogr. Lit. Rev. **30**: 463. doi:10.1016/0198-0254(83)90213-3

370   Arístegui, J., S. Agustí, J. J. Middelburg, and C. M. Duarte. 2005. Respiration in the

371   mesopelagic and bathypelagic zones of the oceans, p. 181–205. *In* P.A. Del Giorgio

372   and P.J. Le B. Williams [eds.], Respiration in Aquatic Systems. Oxford. Univ. Press.

373   doi: 10.1093/acprof:oso/9780198527084.003.0010

374   Azam, F., T. Fenchel, J. Field, J. Gray, L. Meyer-Reil, and F. Thingstad. 1983. The

375   Ecological Role of Water-Column Microbes in the Sea. Mar. Ecol. Prog. Ser. **10**: 257–

376   263. doi:10.3354/meps010257

377   Bănaru, D., F. Carlotti, A. Barani, G. Gregori, N. Neffati, and M. Harmelin-Vivien. 2013.

378   Seasonal variation of stable isotope ratios of size-fractionated zooplankton in the Bay

379   of Marseille (NW Mediterranean Sea). J. Plankton Res. **36**: 145–156.

380   doi:10.1093/plankt/fbt083

381   Barnes, C., D. Maxwell, D. Reuman, and S. Jennings. 2010. Global patterns in predator-

382   prey size relationships reveal size dependency of trophic transfer efficiency. Ecology

383   **91**: 222–232. doi:10.1890/08-2061.1

384   Bates, D., M. Mächler, B. Bolker, and S. Walker. 2014. Fitting Linear Mixed-Effects

385   Models using lme4. **67**. doi:10.18637/jss.v067.i01

386   Bode, A., and M. Alvarez-Ossorio. 2004. Taxonomic versus trophic structure of

387   mesozooplankton: a seasonal study of species succession and stable carbon and

388   nitrogen isotopes in a coastal upwelling ecosystem. ICES J. Mar. Sci. **61**: 563–571.

389   doi:10.1016/j.icesjms.2004.03.004

390   Boecklen, W. J., C. T. Yarnes, B. A. Cook, and A. C. James. 2011. On the use of stable

391   isotopes in trophic ecology. Annu. Rev. Ecol. Evol. Syst. **42**: 411–440.

392   doi:10.1146/annurev-ecolsys-102209-144726

393   Botas, J. A., E. Fernández, A. Bode, and R. Anadón. 1989. Water masses off the Central

394   Cantabrian Coast. Sci. Mar. **53**: 755–761.

395   Burd, A. B., D. A. Hansell, D. K. Steinberg, and others. 2010. Assessing the apparent

396   imbalance between geochemical and biochemical indicators of meso- and

397   bathypelagic biological activity: What the @$#! is wrong with present calculations of

398   carbon budgets? Deep. Res. Part II Top. Stud. Oceanogr. **57**: 1557–1571.

399   doi:10.1016/j.dsr2.2010.02.022

400   Cohen, J. E., S. L. Pimm, P. Yodzis, and J. Saldaña. 1993. Body sizes of animal predators

401   and animal prey in food webs. J. Anim. Ecol. **62**: 67–78. doi:10.2307/5483

402 Company, J. B., and F. Sardà. 2000. Growth parameters of deep-water decapod crustaceans
403   in the Northwestern Mediterranean Sea: a comparative approach. Mar. Biol. **136**: 79–
404   90. doi:10.1007/s002270050011

405 Cushing, D. H. 1989. A difference in structure between ecosystems in strongly stratified
406   waters and in those that are only weakly stratified. J. Plankton Res. **11**: 1–13.
407   doi:10.1093/plankt/11.1.1

408 Deuser, W. G. 1986. Seasonal and interannual variations in deep-water particle fluxes in
409   the Sargasso Sea and their relation to surface hydrography. Deep Sea Res. Part A.
410   Oceanogr. Res. Pap. **33**: 225–246. doi:10.1016/0198-0149(86)90120-2

411 Dilling, L., and A. L. Alldredge. 2000. Fragmentation of marine snow by swimming
412   macrozooplankton: A new process impacting carbon cycling in the sea. Deep. Res.
413   Part I Oceanogr. Res. Pap. **47**: 1227–1245. doi:10.1016/S0967-0637(99)00105-3

414 Espinasse, B., M. Harmelin-Vivien, M. Tiano, L. Guilloux, and F. Carlotti. 2014. Patterns
415   of variations in C and N stable isotope ratios in size-fractionated zooplankton in the
416   Gulf of Lion, NW Mediterranean Sea. J. Plankton Res. **36**: 1204–1215.
417   doi:10.1093/plankt/fbu043

418 Fanelli, E., J. E. Cartes, and V. Papiol. 2011. Food web structure of deep-sea
419   macrozooplankton and micronekton off the Catalan slope: Insight from stable
420   isotopes. J. Mar. Syst. **87**: 79–89. doi:10.1016/j.jmarsys.2011.03.003

421 Färber-Lorda, J. 1994. Length-weight relationships and coefficient of condition of
422   *Euphausia superba* and *Thysanoessa macrura* (Crustacea: Euphausiacea) in south

423   west Indian Ocean during summer. Mar. Biol. **118**: 645–650.

424   Fernández, E., and A. Bode. 1991. Seasonal patterns of primary production in the Central

425   Cantabrian Sea (Bay of Biscay). Sci. Mar. **55**: 629–636.

426   Fry, B., and R. Quiñones. 1994. Biomass spectra and stable isotope indicators of trophic

427   level in zooplankton of the northwest Atlantic. Mar. Ecol. Prog. Ser. **112**: 201–204.

428   doi:10.3354/meps112201

429   Gómez-Ballesteros, M., M. Druet, A. Muñoz, and others. 2014. Geomorphology of the

430   Avilés Canyon System, Cantabrian Sea (Bay of Biscay). Deep Sea Res. Part II Top.

431   Stud. Oceanogr. **106**: 99–117. doi:10.1016/j.dsr2.2013.09.031

432   González-Gil, R., F. González Taboada, C. Cáceres, J. L. Largier, and R. Anadón. 2018.

433   Winter-mixing preconditioning of the spring phytoplankton bloom in the Bay of

434   Biscay. Limnol. Oceanogr. **63**: 1264–1282. doi:10.1002/lno.10769

435   Gooday, A. J. 2002. Biological responses to seasonally varying fluxes of organic matter to

436   the ocean floor: A review. J. Oceanogr. **58**: 305–332. doi:10.1023/A:1015865826379

437   Gowing, M. M., and K. F. Wishner. 1998. Feeding ecology of the copepod *Lucicutia aff. L.*

438   *grandis* near the lower interface of the Arabian Sea oxygen minimum zone. Deep. Res.

439   Part II **45**: 2433–2459. doi:10.1016/S0967-0645(98)00077-0

440   Hannides, C. C. S., B. N. Popp, C. Anela Choy, and J. C. Drazen. 2013. Midwater

441   zooplankton and suspended particle dynamics in the North Pacific Subtropical Gyre:

442   A stable isotope perspective. Limnol. Oceanogr. **58**: 1931–1936.

443   doi:10.4319/lo.2013.58.6.1931

444   Hannides, C. C. S., B. N. Popp, M. R. Landry, and B. S. Graham. 2009. Quantification of

445   zooplankton trophic position in the North Pacific Subtropical Gyre using stable

446   nitrogen isotopes. Limnol. Oceanogr. **54**: 50–61. doi: 10.4319/lo.2009.54.1.0050

447   Honjo, S., S. J. Manganini, and J. J. Cole. 1982. Sedimentation of biogenic matter in the

448   deep ocean. Deep. Res. Part I-Oceanographic Res. Pap. **29**: 609–625.

449   doi:10.1016/0198-0149(82)90079-6

450   Ingram, T., B. Matthews, C. Harrod, T. Stephens, J. Grey, R. Markel, and A. Mazumder.

451   2007. Lipid extraction has little effect on the δ^{15}N of aquatic organisms. Limnol.

452   Oceanogr. Methods **5**: 338–343. doi:10.4319/lom.2007.5.338

453   Jennings, S., C. Barnes, J. Sweeting, and N. V. C. Polunin. 2008a. Application of nitrogen

454   stable isotope analysis in size-based marine food web and macroecological research.

455   Rapid Commun. Mass Spectrom. **22**: 1673–1680. doi:10.1002/rcm

456   Jennings, S., and N. Dulvy. 2005. Reference points and reference directions for size-based

457   indicators of community structure. ICES J. Mar. Sci. **62**: 397–404.

458   doi:10.1016/j.icesjms.2004.07.030

459   Jennings, S., T. Maxwell, M. Schratzberger, and S. Milligan. 2008b. Body-size dependent

460   temporal variations in nitrogen stable isotope ratios in food webs. Mar. Ecol. Prog.

461   Ser. **370**: 199–206. doi:10.3354/meps07653

462   Jennings, S., J. A. A. De Oliveira, and K. J. Warr. 2007. Measurement of body size and

463   abundance in tests of macroecological and food web theory. J. Anim. Ecol. **76**: 72–82.

464   doi:10.1111/j.1365-2656.2006.01180.x

465   Jennings, S., J. Pinnegar, N. Polunin, and K. Warr. 2002. Linking size-based and trophic

466   analyses of benthic community structure. Mar. Ecol. Prog. Ser. **226**: 77–85.

467   doi:10.3354/meps226077

468   Koppelmann, R. 2003. Vertical distribution of mesozooplankton and its δ^{15}N signature at a

469   deep-sea site in the Levantine Sea (eastern Mediterranean) in April 1999. J. Geophys.

470   Res. **108**: 8118. doi:10.1029/2002JC001351

471   Koppelmann, R., R. Böttger-Schnack, J. Möobius, and H. Weikert. 2009. Trophic

472   relationships of zooplankton in the eastern Mediterranean based on stable isotope

473   measurements. J. Plankton Res. **31**: 669–686. doi:10.1093/plankt/fbp013

474   Koppelmann, R., and H. Weikert. 1999. Temporal changes of deep-sea mesozooplankton

475   abundance in the temperate NE Atlantic and estimates of the carbon budget. Mar.

476   Ecol. Prog. Ser. **179**: 27–40. doi:10.3354/meps179027

477   Kürten, B., I. Frutos, U. Struck, S. J. Painting, N. V. C. Polunin, and J. J. Middelburg.

478   2013. Trophodynamics and functional feeding groups of North Sea fauna: A combined

479   stable isotope and fatty acid approach. Biogeochemistry **113**: 189–212.

480   doi:10.1007/s10533-012-9701-8

481   Laakmann, S., and H. Auel. 2010. Longitudinal and vertical trends in stable isotope

482   signatures (δ^{13}C and δ^{15}N) of omnivorous and carnivorous copepods across the South

483   Atlantic Ocean. 463–471. doi:10.1007/s00227-009-1332-9

484   Layman, C., K. Winemiller, D. Arrington, and D. Jepsen. 2005. Body size and trophic

485   position in a diverse tropical food web. Ecology **86**: 2530–2535. doi:10.1890/04-1098

486   Legendre, L., and F. Rassoulzadegan. 1995. Plankton and nutrient dynamics in marine

487   waters. Ophelia **41**: 153–172. doi:10.1080/00785236.1995.10422042

488   Matthews, B., and A. Mazumder. 2005. Consequences of large temporal variability of

489   zooplankton δ^{15}N for modeling fish trophic position and variation. **50**: 1404–1414.

490   doi:doi.org/10.4319/lo.2005.50.5.1404

491   Middelburg, J. J. 2014. Stable isotopes dissect aquatic food webs from the top to the

492   bottom. Biogeosciences **11**: 2357–2371. doi:10.5194/bg-11-2357-2014

493   Minagawa, M., and E. Wada. 1984. Stepwise enrichment of ^{15}N along food chains: Further

494   evidence and the relation between δ^{15}N and animal age. Geochim. Cosmochim. Acta

495   **48**: 1135–1140. doi:10.1016/0016-7037(84)90204-7

496   Mintenbeck, K., U. Jacob, R. Knust, W. E. Arntz, and T. Brey. 2007. Depth-dependence in

497   stable isotope ratio δ^{15}N of benthic POM consumers: The role of particle dynamics

498   and organism trophic guild. Deep Sea Res. Part I Oceanogr. Res. Pap. **54**: 1015–1023.

499   doi:10.1016/j.dsr.2007.03.005

500   Nakagawa, S., and H. Schielzeth. 2013. A general and simple method for obtaining R^2 from

501   generalized linear mixed-effects models R.B. O'Hara [ed.]. Methods Ecol. Evol. **4**:

502   133–142. doi:10.1111/j.2041-210x.2012.00261.x

503   Nakazawa, T., Y. Sakai, C. Hsieh, T. Koitabashi, I. Tayasu, N. Yamamura, and N. Okuda.

504   2010. Is the relationship between body size and trophic niche position time-invariant

505   in a predatory fish? First stable isotope evidence. PLoS One **5**: e9120.

506   doi:10.1371/journal.pone.0009120

507 O'Reilly, C. M., and R. E. Hecky. 2002. Interpreting stable isotopes in food webs:

508   recognizing the role of time averaging at different trophic levels. Limnol. Oceanogr.

509   **47**: 306–309. doi:10.4319/lo.2002.47.1.0306

510 Peters, R. H. 1983. The ecological implications of body size, Cambridge University Press.

511 Polunin, N. V. C., B. Morales-Nin, W. E. Pawsey, J. E. Cartes, J. K. Pinnegar, and J.

512   Moranta. 2001. Feeding relationships in Mediterranean bathyal assemblages

513   elucidated by stable nitrogen and carbon isotope data. Mar. Ecol. Prog. Ser. **220**: 13–

514   23. doi:10.3354/meps220013

515 Robinson, C., D. K. Steinberg, T. R. Anderson, and others. 2010. Mesopelagic zone

516   ecology and biogeochemistry - A synthesis. Deep. Res. Part II Top. Stud. Oceanogr.

517   **57**: 1504–1518. doi:10.1016/j.dsr2.2010.02.018

518 Rolff, C. 2000. Seasonal variation in δ^{13}C and δ^{15}N of size-fractionated plankton at a

519   coastal station in the northern Baltic proper. Mar. Ecol. Prog. Ser. **203**: 47–65.

520   doi:10.3354/meps203047

521 Romero-Romero, S., A. Molina-Ramírez, J. Höfer, and J. L. Acuña. 2016a. Body size-

522   based trophic structure of a deep marine ecosystem. Ecology **97**: 171–181.

523   doi:10.1890/15-0234.1

524   Romero-Romero, S., A. Molina-Ramírez, J. Höfer, G. Duineveld, A. Rumín-Caparrós, A.

525   Sanchez-Vidal, M. Canals, and J. L. Acuña. 2016b. Seasonal pathways of organic

526   matter within the Avilés submarine canyon: Food web implications. Deep Sea Res.

527   Part I Oceanogr. Res. Pap. **117**: 1–10. doi:10.1016/j.dsr.2016.09.003

528   Rumín-Caparrós, A., A. Sanchez-Vidal, C. González-Pola, G. Lastras, A. Calafat, and M.

529   Canals. 2016. Particle fluxes and their drivers in the Avilés submarine canyon and

530   adjacent slope, central Cantabrian margin, Bay of Biscay. Prog. Oceanogr. **144**: 39–

531   61. doi:10.1016/j.pocean.2016.03.004

532   Saino, T., and A. Hattori. 1980. ^{15}N natural abundance in oceanic suspended particulate

533   matter. Nature **283**: 752–754. doi:10.1038/283752a0

534   Sheldon, R. W., A. Prakash, and H. Sutcliffe. 1972. The size distribution of particles in the

535   ocean. Limnol. Oceanogr. **17**: 327–340. doi:10.4319/lo.1972.17.3.0327

536   Sheldon, R. W., W. H. Sutcliffe Jr., and M. A. Paranjape. 1977. Structure of pelagic food

537   chain and relationship between plankton and fish production. J. Fish. Res. Board

538   Canada **34**: 2344–2353. doi:10.1139/f77-314

539   Steinberg, D. K., B. A. S. Van Mooy, K. O. Buesseler, P. W. Boyd, T. Kobari, and D. M.

540   Karl. 2008. Bacterial vs. zooplankton control of sinking particle flux in the ocean's

541   twilight zone. Limnol. Oceanogr. **53**: 1327–1338.

542   doi:doi.org/10.4319/lo.2008.53.4.1327

543   Takahashi, K., A. Kuwata, H. Sugisaki, K. Uchikawa, and H. Saito. 2009. Downward

544   carbon transport by diel vertical migration of the copepods *Metridia pacifica* and

545   *Metridia okhotensis* in the Oyashio region of the western subarctic Pacific Ocean.

546   Deep. Res. Part I Oceanogr. Res. Pap. **56**: 1777–1791. doi:10.1016/j.dsr.2009.05.006

547   Team, R. C. 2015. R: A Language and Environment for Statistical Computing. Vienna,

548   Austria: R Foundation for Statistical Computing.

549   Turner, J. T. 2015. Zooplankton fecal pellets, marine snow, phytodetritus and the ocean's

550   biological pump. Prog. Oceanogr. **130**: 205–248. doi:10.1016/j.pocean.2014.08.005

551   Uye, S. 1982. Length-weight relationships of important zooplankton from the inland Sea of

552   Japan. J. Oceanogr. Soc. Japan **38**: 149–158.

553   Wilson, S. E., D. K. Steinberg, and K. O. Buesseler. 2008. Changes in fecal pellet

554   characteristics with depth as indicators of zooplankton repackaging of particles in the

555   mesopelagic zone of the subtropical and subarctic North Pacific Ocean. Deep. Res.

556   Part II Top. Stud. Oceanogr. **55**: 1636–1647. doi:10.1016/j.dsr2.2008.04.019

557   Woodward, G., B. Ebenman, M. Emmerson, J. M. Montoya, J. M. Olesen, A. Valido, and

558   P. H. Warren. 2005. Body size in ecological networks. Trends Ecol. Evol. **20**: 402–9.

559   doi:10.1016/j.tree.2005.04.005

560   Zuur, A. F., E. N. Ieno, N. J. Walker, A. A. Saveliev, and G. M. Smith. 2009. Mixed

561   Effects Models and Extensions in Ecology with R, M. Gail, K. Krickeberg, J.M.

562   Samet, A. Tsiatis, and W. Wong [eds.]. Springer.

563

564

565   **Tables**

566   Table 1. Hydrographic conditions, pathways of organic matter OM and particle flux in each
567   BIOCANT cruise.

| Oceanographic period	Cruise	Hydrographic conditions	Pathways of OM and particle flux
Onset spring bloom	March 2012, BIOCANT 1	High surface Chl *a* concentration. Vertical mixing.	Predominance of OM produced by phytoplankton in Surface Water (SW). Refractory suspended OM below SW from the previous production cycle and of terrigenous origin.
Late stratification	October 2012, BIOCANT 2	Low Chl *a* concentration. Thermocline of 6ºC gradient.	Suspended OM in the water column similar to the early stratification period (see below). Low mass flux.
Early stratification	May 2013, BIOCANT 3	Subsurface Chl *a* maximum. Thermocline of 2ºC gradient.	Suspended OM is homogeneous along the water column after the produced OM in the spring phytoplankton bloom has sank.

568

569

570 **Figures**
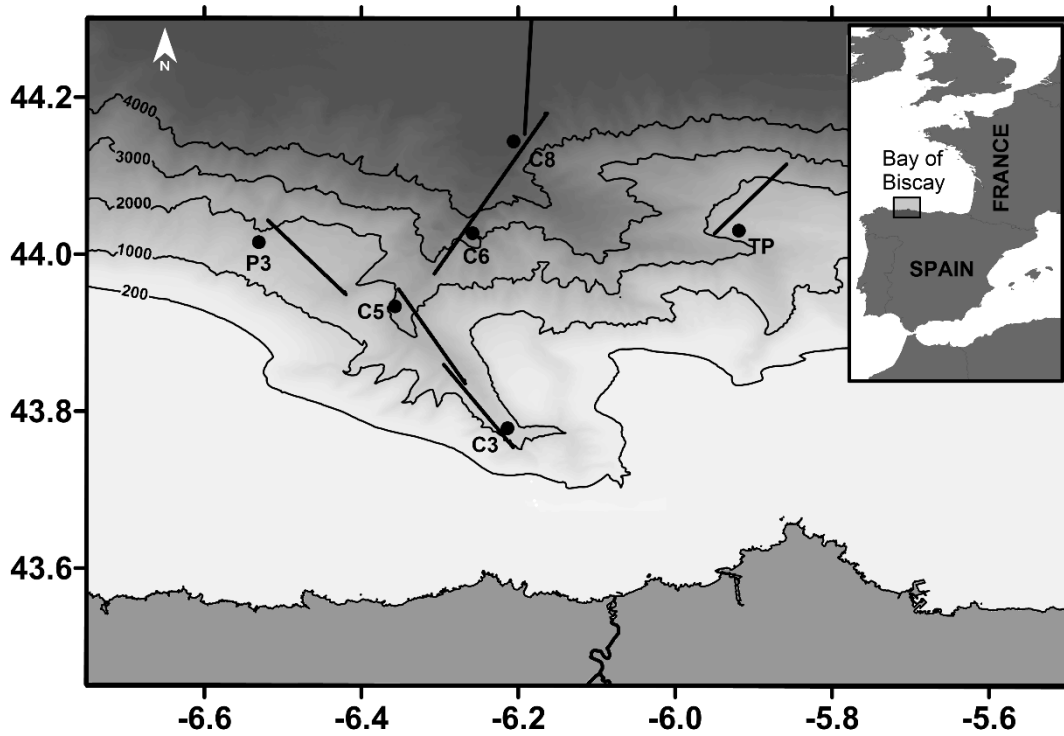
572 Figure 1. Map of the study area. Dots indicate locations of stations and lines refer to the

573 trawling of the MOCNESS net.

574

575
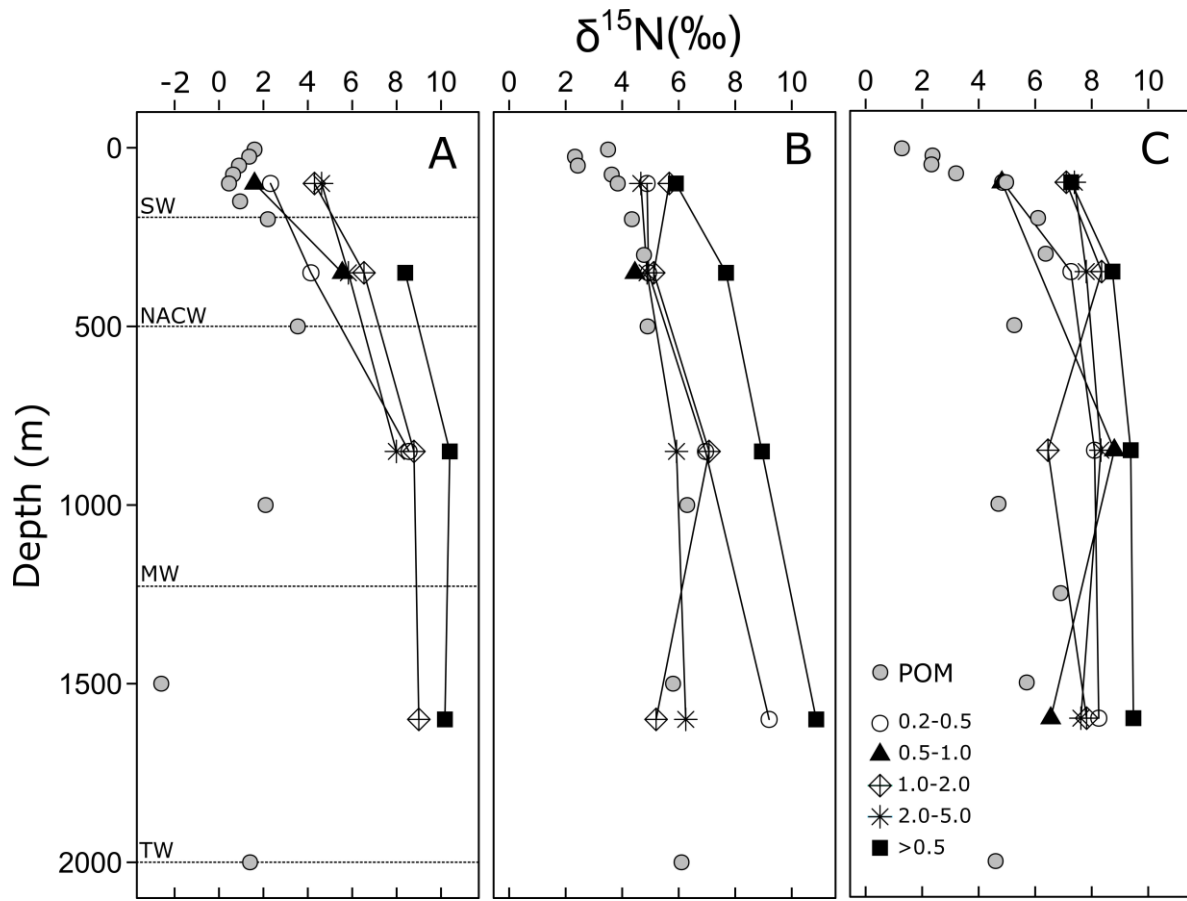
Figure 2. δ^{15}N values of size-fractionated zooplankton and suspended POM collected in

each BIOCANT cruise: A) Onset of spring bloom, March 2012, BIOCANT 1; B) Early

stratification, May 2013, BIOCANT 3; C) Late stratification, October 2012, BIOCANT 2.

Each dot corresponds to the average between all stations at the mean depth of each water

mass (SW: Surface Water; NACW: North Atlantic Central Water; MW: Mediterranean

Water; TW: Transition Water). Horizontal dotted lines demarcate each water mass.

Zooplankton size fractions are given in mm. Note different scale on x-axis.

583
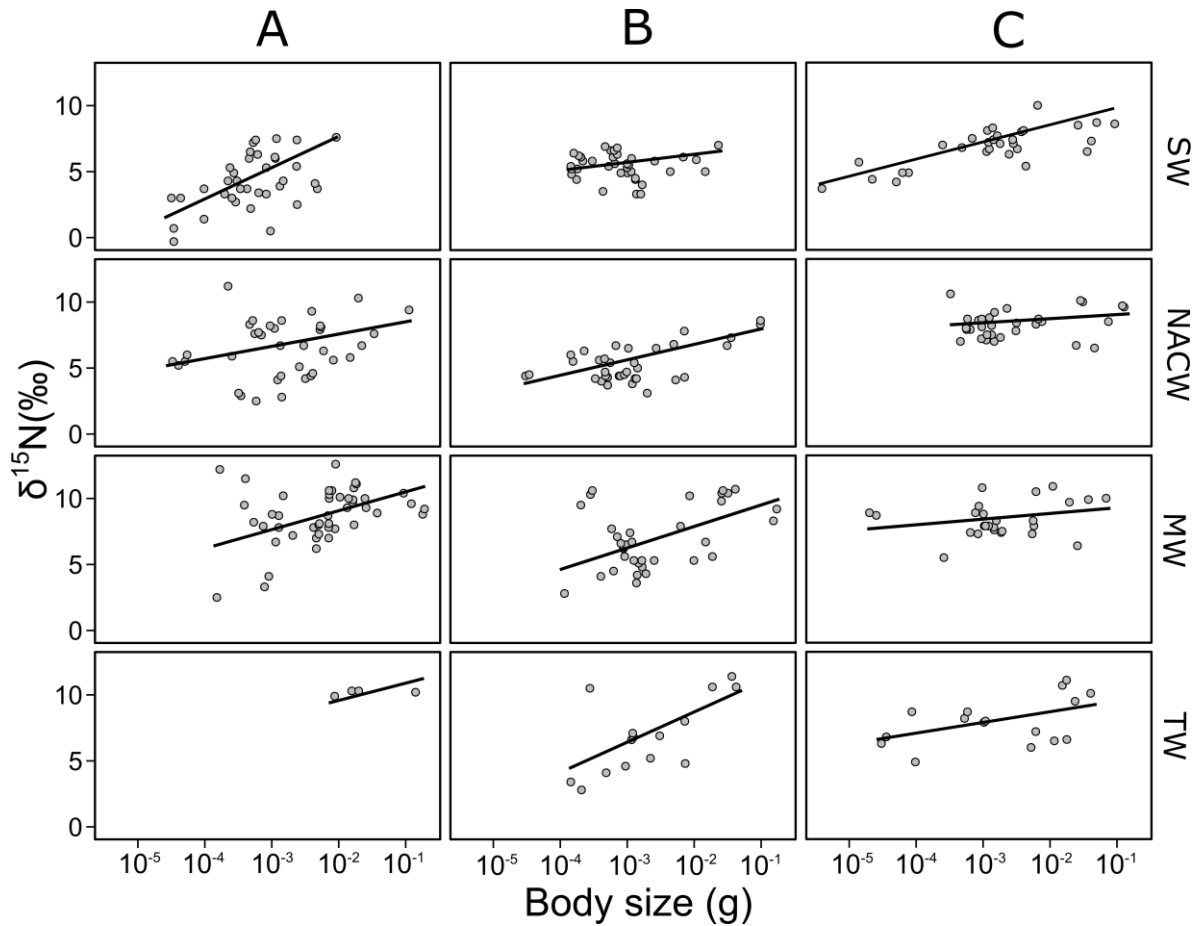
584

585   Figure 3. Relationship between $\delta^{15}N$ and $\log_{10} W$ for each cruise (A: Onset of spring

586   bloom, March 2012, BIOCANT 1; B: Early stratification, May 2013, BIOCANT 3; C: Late

587   stratification, October 2012, BIOCANT 2) and depth strata (SW: Surface Water; NACW:

588   North Atlantic Central Water; MW: Mediterranean Water; TW: Transition Water) fitted

589   from the selected linear mixed model (see material and methods section and Supporting

590   Information).

591

592
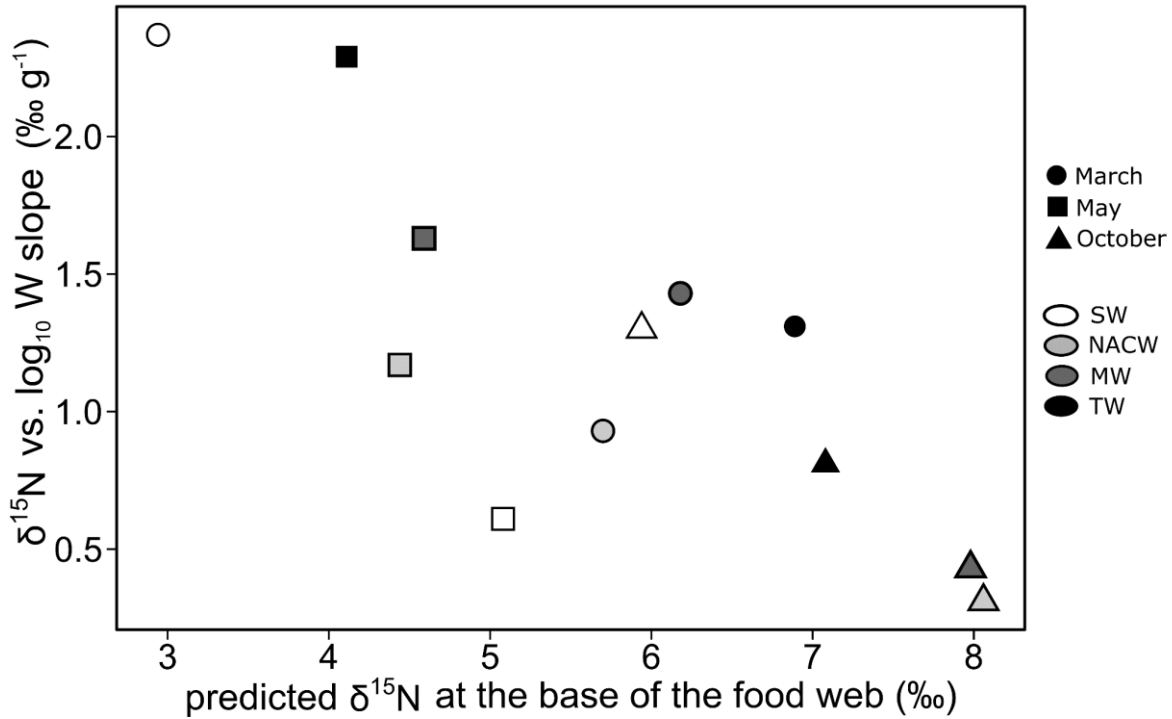
Figure 4. Slope and predicted δ^{15}N values for zooplankton at the base of the studied food

web (i.e. organisms weighing 10^{-4} g) estimated from the best model for the δ^{15}N vs. $\log_{10}$ W

relationship (Fig. 3) for each cruise (onset of spring bloom, March 2012, BIOCANT 1;

early stratification, May 2013, BIOCANT 3; late stratification, October 2012, BIOCANT

2) and depth strata (SW: Surface Water; NACW: North Atlantic Central Water; MW:

Mediterranean Water; TW: Transition Water).